High order Finite Elements for mid-frequency vibro-acoustics

F. Frischmann[1], S. Kollmannsberger[1], A. Rabold[2], E. Rank[1]
[1]Computation in Engineering, Faculty of Civil, Geo and Environmental Engineering,
Technische Universität München, Arcisstr. 21, 80333 München, Germany
[2]ift Rosenheim GmbH, Theodor-Gietl-Str.7-9, 83026 Rosenheim, Germany
email: {frischmann; kollmannsberger; rank}@cie.bgu.tum.de, rabold@ift-rosenheim.de

ABSTRACT: The quantification of vibroacoustic properties in multi-floor timber buildings is currently still based on measurements and computational models are rarely used in practice. One reason surely is a lack of validated and robust numeric schemes for vibro-acoustic simulations covering mid-range frequencies which can be integrated smoothly into the planning process of multi-floor timber buildings. To this end, we lay out a pipeline for the prediction of mid-frequency vibro-acoustic behavior of laminated timber constructions by modal analysis using three-dimensional high-order finite elements. The integration into the planning process is achieved by deriving the computational model from IFC-based building information models.

KEY WORDS: High-order finite elements, vibro-acoustics, building information modeling, laminated timber constructions, hexahedral mesh generation.

1 INTRODUCTION

The prediction of vibro-acoustic properties is of major importance for multi-floor timber buildings due to their lightweight character. Commonly used prediction models in everyday planning practice are mainly based on measurements of isolated components and exemplary component set-ups. However, the transfer of these measured data sets to the real configuration in a whole building system is not straight forward and might not yield a robust prediction. This motivates the usage of numeric methods as prediction models of vibro-acoustic properties. In a high-frequency range methods like the statistical energy analysis (SEA) are applicable. However, the SEA is known to lead to reliable results for high modal densities only, i.e. if a sufficiently large number of eigenfrequencies and -modes are present within the frequency range of interest. This is not the case for low frequencies. In a low frequency range, classical eigenmode analysis using the widely applied finite element method of low order (h-FEM) is known to be a robust numeric prediction scheme. To the contrary, the mid frequency range is difficult to predict for both methods h-FEM and SEA as it lies in between their upper or lower border of validity, respectively.

The motivation of this contribution is twofold. First, it aims at closing the remaining gap in the mid-frequency range by the application of high-order finite element analysis (p-FEM) for vibro-acoustics. Herein, higher order polynomial shape functions are used to discretize the unknowns instead of piecewise low-order shape functions used for classical h-FEM. The use of p-FEM in vibro-acoustic analysis of timber beam floors in combination with proper mesh design has already been shown to form an efficient and accurate numeric scheme [1][4]. This contribution will show the benefits of truly solid p-FEM for vibro-acoustic problems for laminated timber constructions.

The second aim of our research is to demonstrate how vibro-acoustic analysis may smoothly be integrated into the overall planning process using building information models (BIM). A crucial point in this context is the need of highly automated tools for the generation of simulation models from digital building information models.

2 BIM-COUPLED VIBRO-ACOUSTIC SIMULATION PIPELINE

A vibro-acoustic simulation pipeline will be presented in the sequel whose principle components are depicted in Figure 1.

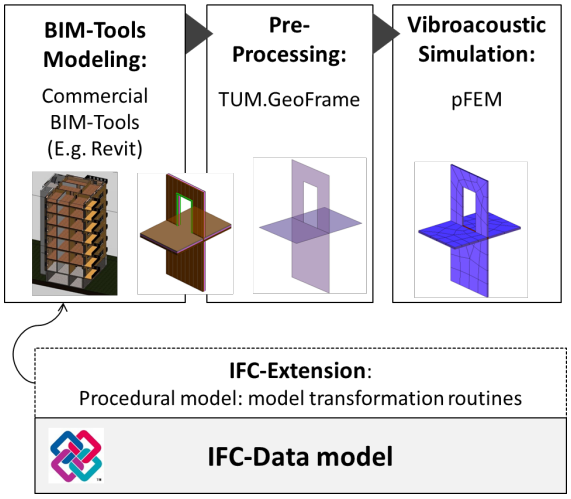

Figure 1: Software components for vibro-acoustic simulation used within this contribution

Starting point is a building information model in form of an industry-foundation-class (IFC)-data model generated in the commercial BIM tool Revit®. This BIM model forms the basis of the generation of a valid computational model. The BIM model is then passed to the TUM.GeoFrame [11] framework (modular structure see Figure 2) which carries out all necessary pre-processing steps. In this step, TUM.GeoFrame first utilizes the open source library

IfcOpenShell [16] to interpret the BIM model topologically and geometrically before it carries out mesh generation in a second step. The complete FE simulation model including all necessary material definitions and boundary condition specifications are then delivered to the high-order FEM code AdhoC.
This general software environment provides the framework to carry out classical modal analysis for typical timber constructions and it provides the potential to treat entire building configurations in order to investigate their vibro-acoustic properties.

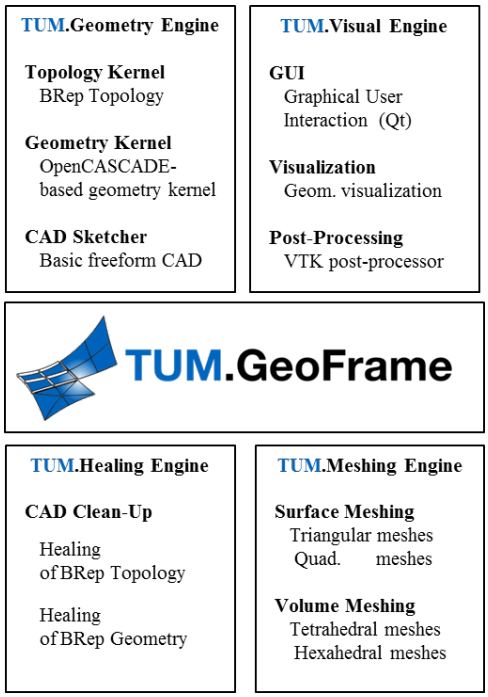

Figure 2: The modular TUM.GeoFrame framework

Two key components in this pipeline are laid out in more detail in the following subsections, in subsection 2.1 how to generate a valid computational geometry from BIM and in subsection 2.2 how to generate three-dimensional hexahedral meshes compatible at the interface of the components. The problem of how to perform a p-FEM eigenvalue analysis is then treated in Section 3.

2.1 Building Information Models and BIM-coupled vibro-acoustic simulations

Building information modeling is a modern approach to tackle the complexity of the engineering planning process in the construction industry. A building information model can be seen as a 3D geometry based database for a building, its components, materials and architectural spaces as well as related processes and planning documentation over the entire lifecycle. This general approach results in an extensive data model to describe buildings.

In this contribution the IFC (industry foundation classes) specification for building information models is utilized. IFC is developed by the buidingSMART organization [15], widely accepted, and used in the architectural and civil engineering modeling community. The IFC data model is standardized according to ISO 16739:2013. The implementation is realized via EXPRESS- and XML-language. The main characteristic is the complex hierarchical structure to describe a building and its components logically, semantically and geometrically. All building components (e.g. walls, slabs, windows) are grouped under a general "IfcBuildingElement" type. IFC is also capable of defining and storing Boolean-type geometric relations of components as illustrated in Figure 3 for a wall-window example.

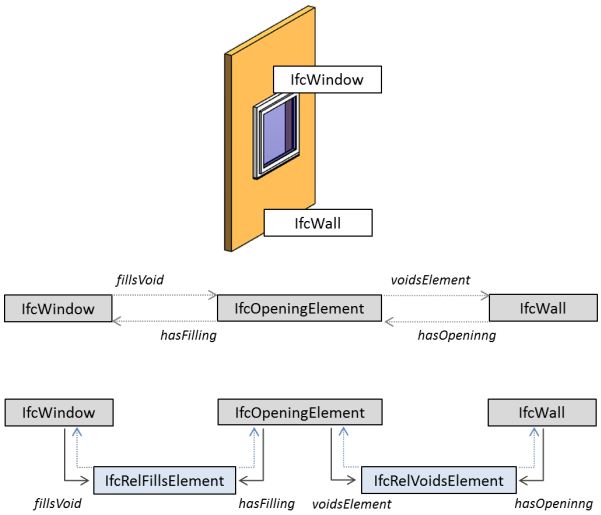

Figure 3: IFC Boolean-type wall-window example

A BIM-based planning approach has many advantages over a classical 2D floor plan based planning process. A BIM model is always based on a 3D model, such that spatial relations and possible spatial conflicts can be detected and resolved directly. A strict BIM approach goes beyond a pure 3D model due to the description of semantics, logical information, and the additional possibility to extend the model by time information. This fact allows for a derivation of lower dimensional plans for documentation and legal regulations from BIM models.
However, the generality of the IFC model is also a drawback in the usage of the building model for structural or numerical simulation during the planning process. A direct usage of a BIM model as a simulation model is not applicable in general, since a BIM model rarely meets the specific model requirements of a simulation models, e.g. for vibro-acoustic FEA. Moreover, up to date BIM models and simulations models are at best treated as weakly *linked* and mostly are independent models in a multi-model approach.
By contrast, this contribution advocates a model-*coupling* approach. Herein, the BIM model is the central model which is bi-directionally coupled to all simulation models. The coupling information includes the model transfers by means of procedural construction steps as well as the final explicit simulation model. This approach allows a robust and efficient model update for the BIM and simulation model likewise.
Figure 4 and Figure 5 illustrate the procedural steps during the transition of a representative component connection in laminated timber from a 3D BIM-model to a valid 2 ½ D model as required for the numerical simulation and finally its discrete, three-dimensional FE mesh.

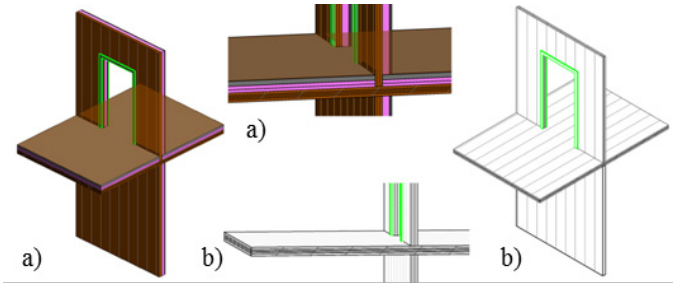

Figure 4: a) BIM model with Boolean-type relation (i.e. door in wall). b) BIM model of structural components only

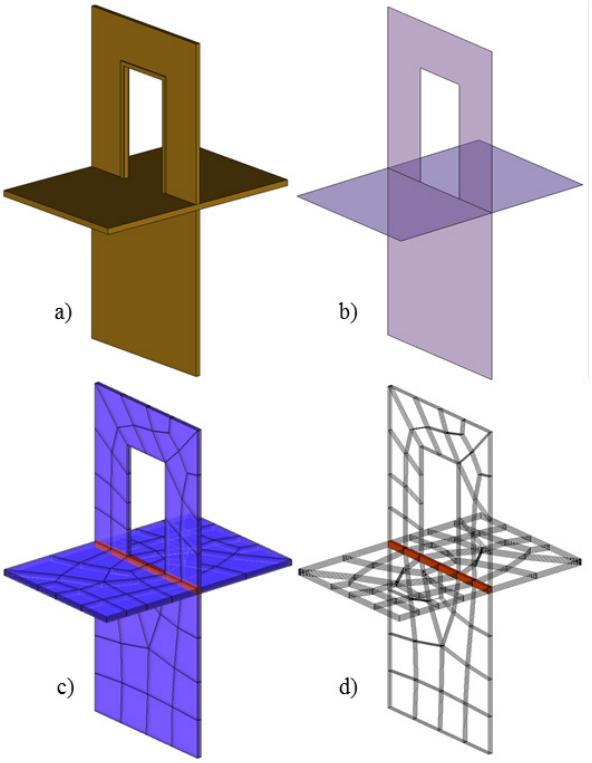

Figure 5: Geometric Models and FE mesh: a) Solid model. b) Topologically consistent 2 ½ D model. c) and d) FE mesh with highlighted multi-shell mesh interface (red).

The necessary procedural steps for the model transition from BIM to 2 ½ D BRep of this specific example are:

1. Build solid boundary representation (BRep) model from IFC data structure:
   a) Conversion of non-BRep data (e.g. CSG) to BRep
   b) Resolving Boolean operations, e.g. of wall-door relations
2. Reduce BRep model to mid-surface representation
3. Ensure geometric and topological connectivity of surfaces
4. Attach thickness, extrusion and layer information to 2 ½ D model
5. Assign material parameters

To store these procedural steps in the IFC data model, an extension of the IFC specification is proposed by the authors. All further implementation issues and technical details of this approach are omitted here as not to exceed the requested format of this paper. Instead, we refer to [9] for details.

The detour from a 3D BIM-model via a 2 ½ D simulation model back to 3D all hexahedral mesh will turn out to pay off as it drastically simplifies the process of mesh generation described in the following.

2.2 Hexahedral Mesh Generation

In civil engineering applications classical finite elements in combination with dimensionally reduced shell models are widely used and have proven to be robust and sufficiently accurate to describe many mechanical problems in this field.

However, an accurate prediction of the complex three dimensional vibro-acoustic effects at the connection of structural components made of laminated timber can hardly be captured by classical dimensionally reduced shell models.

Figure 6a) depicts a fully three-dimensional, all hexahedral finite element mesh of a typical slab-wall connection made of laminated timber while Figure 6b) shows its two-dimensional counterpart.

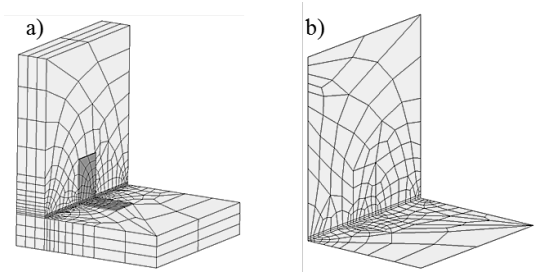

Figure 6: a) Truly three-dimensional all-hexahedral FE mesh. b) Dimensional reduced quadrilateral FE mesh

It is difficult to capture vibro-acoustic effects in junctions of this type by a computational model relying on a dimensionally reduced mesh as an accurate condensation of the 3D mechanical effects onto a 2D representation is neither straight forward nor possible a priori. Therefore, we advocate a strictly three dimensional approach for a vibro-acoustic simulation of laminated timber structures.

Whereas all-quadrilateral surface mesh generation is nowadays possible even for topologically difficult configurations, all-hexahedral meshes for arbitrary volumes are often difficult to create. This is still an active field of research.

However, the complexity of mesh generation can be reduced noticeably for special volume types like volumes of revolution or thin-walled structures. Fortunately, laminated timber structures can be represented by shell-like solid models, a fact used within this contribution to apply all-hexahedral meshing techniques based on extrusion and sweeping of quadrilateral surface meshes.

Extrusion based hexahedral meshing techniques require a representative surface model similar to classical surface meshing techniques. Figure 7 depicts the compatible set of models for FE simulation within which we use the 2 ½ D representation to simplify the meshing process.

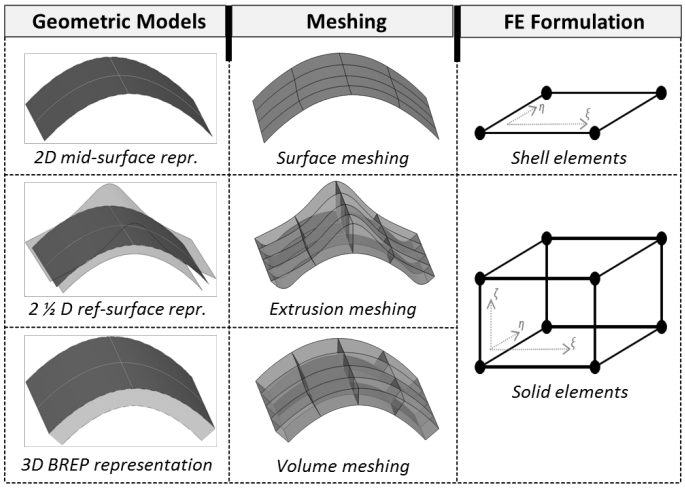

Figure 7: Compatible model set Modeling-Meshing-FEM

The computational advantages of higher-order p-FEM regarding efficiency and accuracy can only be exploited in combination with a proper mesh design. In contrast to h-FEM, p-FEM calls for less mesh elements. This naturally yields larger aspect ratios within finite elements which, fortunately, pose no problem to the high-order formulation. A suitable mesh generator for p-FEM must exploit this fact. TUM.GeoFrame is able to generate meshes, highly suitable for p-FEM. Coarse, high-quality meshes can even be generated in the presence of small features like holes due to its built-in adaptivity and mapping techniques applied at curved surfaces. An example is depicted in Figure 8.

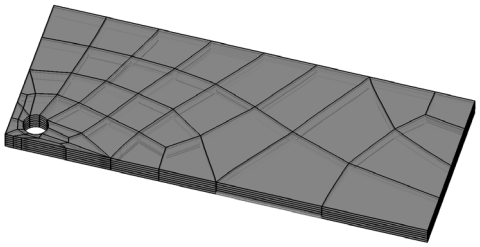

Figure 8: Coarse high-quality FE mesh with small features (i.e. hole in plate) for high-order FEA

However, hexahedral meshing algorithms using only simple extrusion and sweeping techniques on all-quadrilateral surface meshes are only suitable for single-solid-shell models as the one depicted in Figure 8. Multi-shell solid models require a further consideration of the shell intersections for the generation of all-conforming meshes. Figure 9 depicts some of the multi-solid-shell hexahedral meshing templates available in TUM.GeoFrame. We refer to [10][11] for an in-depth description.

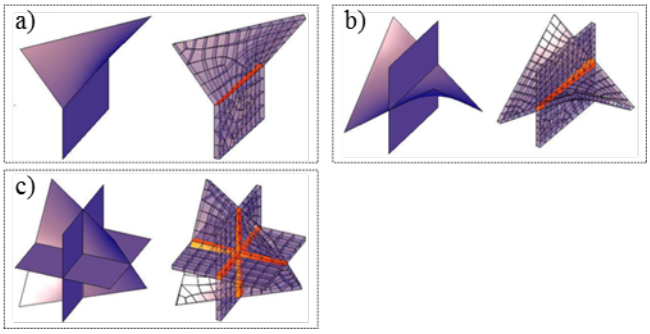

Figure 9: Exemplary conforming multi-shell hex-meshing templates a) b) c).

3 HIGH-ORDER FEM VIBRO-ACOUSTICS

With an analysis suitable mesh at hand, we may now carry out modal analysis by the Bubnov-Galerkin finite element method of high order (p-FEM) which we review briefly for vibro-acoustics in this section.

3.1 The Bubnov-Galerkin finite element method of high order (p-FEM)

The Bubnov-Galerkin finite element method is based on the discretization of the variational or weak formulation of the differential equations for elastodynamic problems, which reads:

$$\int_\Omega \{\overline{w}\}^T \rho_s \frac{d^2}{dt^2}\{u\}dV + \int_\Omega ([D]\{\overline{w}\})^T [A][D]\{u\}dV = \int_{\partial\Omega} \{\overline{w}\}^T \{t\}dS + \int_\Omega \{\overline{w}\}^T \{b\}dV \quad (1)$$

Discretized by properly defined ansatz functions N and discrete field variables for the unknown displacements u and the weighting functions w yields:

$$\{u\} \approx [N]_S \{\widetilde{u}\}$$
$$\frac{d^2}{dt^2} \approx [N]_S \{\ddot{\widetilde{u}}\} \quad (2)$$
$$\{\overline{w}\} \approx [N]_S \{\widetilde{w}\}; \{\overline{w}\}^T = \{\overline{w}_x, \overline{w}_y, \overline{w}_z\}$$

The discretized weak formulation results in a system of equation for the system (denoted by $^{(s)}$) assembled of finite discrete elements $V^{(e)}$.

$$[M]_s^{(s)} \{\ddot{\widetilde{u}}\} + [K]_s^{(s)} \{\widetilde{u}\} = \{F\}^{(s)} \quad (3)$$

$[M]_s$ is the mass matrix and $[K]_s$ the stiffness matrix of the entire system, assembled from a finite number of volume elements. For one volume element $V^{(e)}$ with bounding surface $S^{(e)}$ the mass matrix $[M]_s$ and stiffness matrix $[K]_s$ read:

$$[K]_s^{(e)} = \int_{V_{(e)}} ([D][N]_s)^T [A][D][N]_s \, dV$$
$$[M]_s^{(e)} = \int_{V_{(e)}} [N]_s{}^T \rho_s [N]_s \, dV \quad (4)$$

The right-hand side force vector {F} is composed of internal and external forces and reads:

$$\{F\}^{(e)} = \int_{S^{(e)}} [N]_s{}^T \{t\} dS + \int_{V^{(e)}} [N]_s{}^T \{b\} dV \quad (5)$$

The dynamic problem (formula (3)) can be solved in the frequency domain by transformation to an eigenvalue problem, considering only homogenous boundary conditions.

A Fourier series ansatz for the displacements u yields the final eigenvalue formulation of the problem including the eigenvectors {φ} and the scaling factors $q_{i,n}$:

$$\tilde{u}(x,y,z,t) = \sum_{n=-\infty}^{\infty} \sum_{i=1}^{n_{dof}} \varphi_i(x,y,z) q_{i,n} e^{jw_i t}$$
$$([K]_s - w^2 [M]_s)\{u\}_n = 0 \quad (6)$$

Every degree of freedom of the system is linked to one eigenvector φ_i and one circular eigenfrequency w_i of the system.

$$([K]_s - w_i^2 [M]_s)\{\varphi\}_i = 0 \quad (7)$$

The eigenvalue problem of the unloaded structure gives an insight into the vibroacoustic properties. The eigenfrequencies and eigenvectors of the system can, for example, be utilized within vibroacoustic simulations, for excitation models or for coupled sound radiation simulations as in [7][8].

3.2 High-order p-version finite element method

The accuracy of the approximated solution of the continuous unknown displacement field is strongly dependent on the definition of suitable ansatz functions defined on discrete degrees of freedom.

$$\{u\} \approx [N]_s \{\tilde{u}\} \quad (8)$$

Whereas the classical h-version of the finite element method uses mainly Lagrange polynomials, the p-version FEM exploits hierarchical functions generated from orthogonal Legendre polynomials. They hold the important property that a set of higher-order shape functions incorporate the shape functions of lower order. The one-dimensional hierarchical shape functions (in-depth described in [1]) are defined as follows:

$$N_1(\xi) = 1/2(1-\xi), N_2(\xi) = 1/2(1+\xi),$$
$$N_i(\xi) = \Phi_{i-1}(\xi), i = 3,4,..., p+1 \quad (9)$$

where $\Phi_j(\xi)$ and the Legendre polynomials L_k read:

$$\Phi_j(\xi) = \sqrt{\frac{2j-1}{2}} \int_{-1}^{\xi} L_{j-1}(x) dx, j = 2,3,..., p \quad (10)$$

$$L_k(x) = \frac{1}{2^k k! dx^k} (x^2-1)^k, x \in (-1,1), k = 0,1,2,... \quad (11)$$

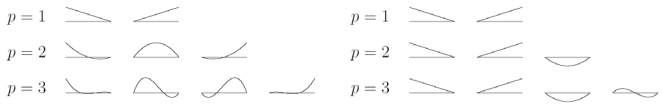

Figure 10: Non-hierarchical 1D-shape functions (left) vs. hierarchical shape functions used for p-FEM (right)

Extensions to higher dimensions are carried out by forming tensor products of one-dimensions. Trunk spaces are possible as well and are especially favorable for thin solid structures, which additionally allow for an orthotropic discretization in which the polynomial degrees in the in-plane directions are chosen higher than the polynomial degree for the thickness direction. A detailed description is given in [2].

4 NUMERICAL RESULTS

In the following we present numerical results for high-order finite element analysis performed on an exemplary wall-slab construction made of laminated timber. The generation of the geometric simulation model and FE mesh for this example on basis of a BIM-model was shown previously and is illustrated in Figure 4 and Figure 5.

All FE computations are performed assuming orthotropic material, defined by the set of material properties, specifically E-moduli E_{xy}, E_{yz}, E_{zx}, shear moduli G_{xy}, G_{yz}, G_{zx} and Poison ratios ν_{xy}, ν_{yz}, ν_{zx}.

These numerical results demonstrate the potential of high-order FEA exemplarily for the wall-slab configuration depicted in Figure 11. The wall consists of 3-layers of 81 mm strong laminated timber elements, with layer thicknesses of [27-27-27] mm. The slab consists of 5-layer 105 mm thick laminated timber elements, with layer thicknesses of [27-17-17-17-27] mm. The orthotropic material properties are obtained by material parameter fits on basis of experimental and numerical test on Leno® 81 and 105 laminated timber test samples respectively, carried out in scope of the research activities at HS Rosenheim and TU München (S. Mecking and C. Winter) [17][18].

The layered material is discretized in thickness direction with one finite element per layer as illustrated in Figure 11. The orthotropic material parameter for material L1 (layers 1 and 3 of the walls and 1, 3, 5 of the slab) and material L2 are given in Table 1.

Mat. L1	Value	
E_{xy}	10,211	[N/mm²]
E_{yz}	1,424	[N/mm²]
E_{zx}	137	[N/mm²]
G_{xy}	459	[N/mm²]
G_{yz}	102	[N/mm²]
G_{zx}	171	[N/mm²]
ν_{xy}, ν_{yz}, ν_{zx}	0.02	[-]

Mat. L1	Value	
E_{xy}	1,424	[N/mm²]
E_{yz}	10,211	[N/mm²]
E_{zx}	459	[N/mm²]
G_{xy}	137	[N/mm²]
G_{yz}	102	[N/mm²]
G_{zx}	171	[N/mm²]
ν_{xy}, ν_{yz}, ν_{zx}	0.02	[-]

Table 1: Orthotropic material properties

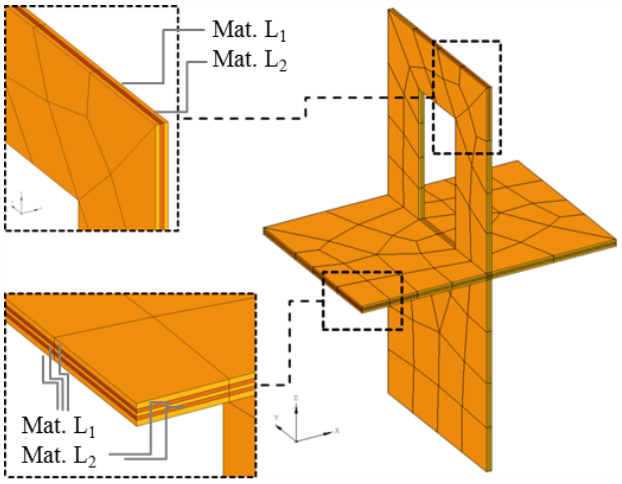

Figure 11: FE mesh and material layers

The displacement boundary conditions for the modal analysis are depicted in Figure 12. The structure is supported in y-direction on all narrow sides of the walls as well as the slab. The structure is further supported in the other spatial directions on the lower wall's downside while symmetry boundary conditions are applied at the slab's narrow side. The upper wall at its top side is additionally supported in x-direction.

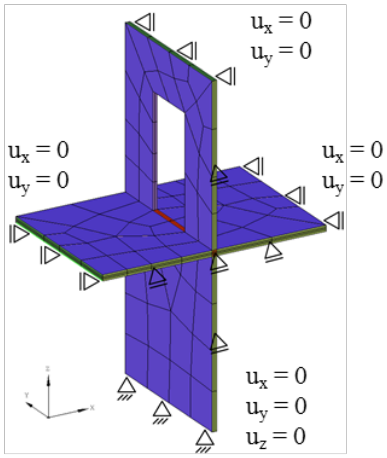

Figure 12: FE System and displacement boundary conditions

The lack of an analytic reference solution is addressed by a highly accurate "overkill solution" (in the sequel denoted by the subscript $_{(ovk)}$) obtained from a p-FEM simulation with about 356,000 degrees of freedom. The distribution of the first 100 computed eigenfrequencies over a frequency range up to 400 [Hz] is given in Figure 13 and Figure 14.

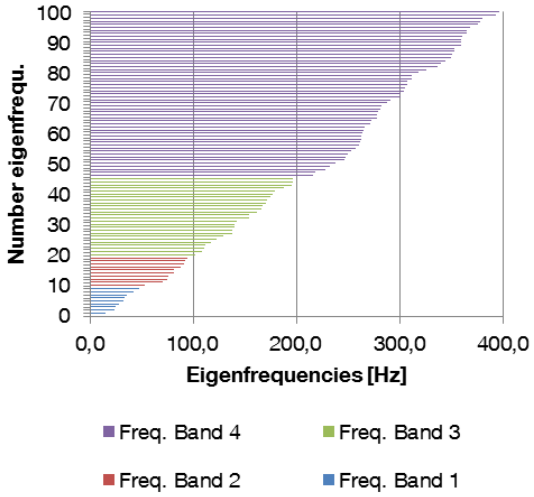

Figure 13: First 100 Eigenfrequencies and assigned frequency bands

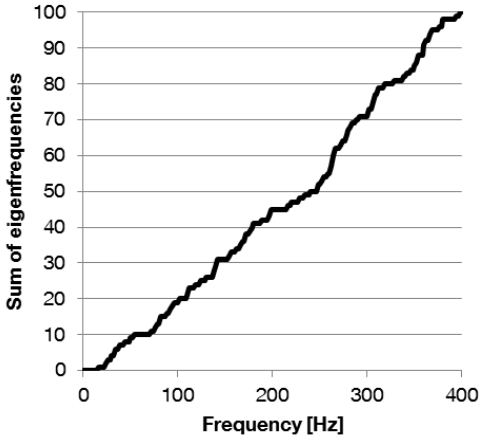

Figure 14: Cumulative distribution of first 100 eigenfrequencies

For the convergence study the frequency range of the first 100 eigenfrequencies is divided into four frequency bands. The first ranges from 0 to 50 [Hz], the second band covers the octave from 50 to 100 [Hz], followed by the octave band in range of 100 to 200 [Hz], and the last section for all frequencies above up to 400 [Hz]. Figure 13 visualizes the increasing modal density in the later frequency octave bands.
From each frequency band one eigenpair result consisting of eigenmode plot and convergence plot comparing the relative error of p-refined p-FEM vs. classical h-refined low-order FEM solution is shown in Figure 16 to Figure 19.
The comparison of h- and p-refinement strategies is carried out on the basis of the meshes depicted in Figure 15. The p-FEM solution is obtained from the first coarse mesh by p-

refinement, whereas the h-FEM solution, using trilinear hexahedral elements is obtained by the illustrated mesh refinements.

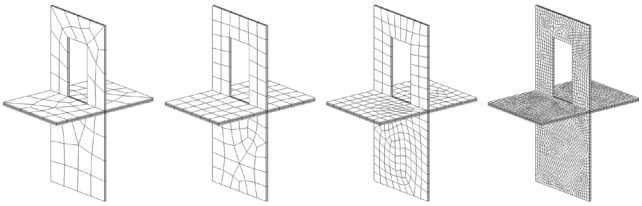

Figure 15: h-refinement meshes

The convergence plots in Figure 16 to Figure 19 depict the relative error w.r.t. the 'reference solution' against the degrees of freedom for p- and h-refinement strategies:

Relative error: $$\varepsilon = \frac{f_{i,FEM} - f_{i,ovk}}{f_{i,ovk}} * 100\% \qquad (12)$$

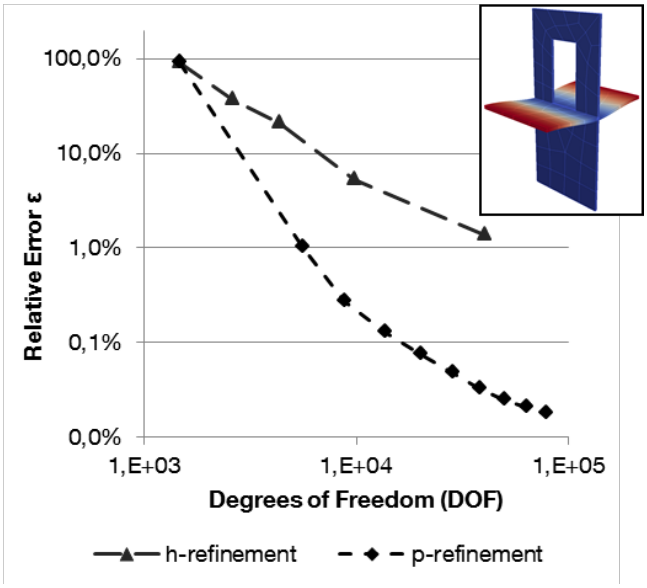

Figure 16: Eigenmode [4] 28.1 Hz

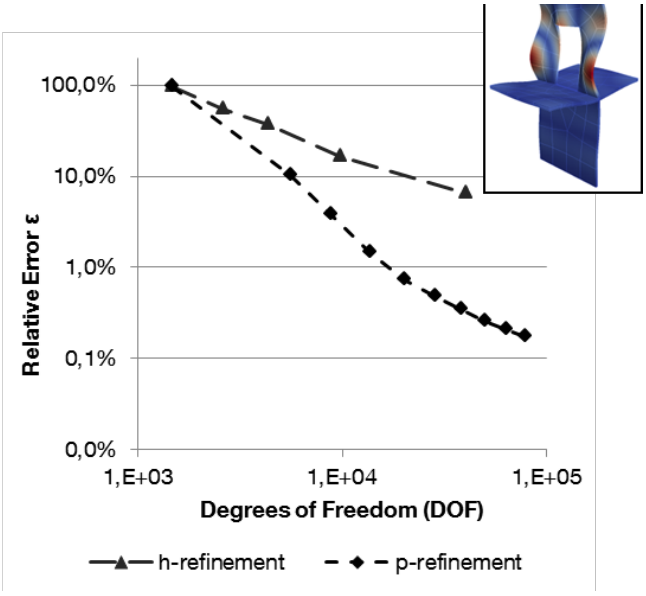

Figure 17: Eigenmode [16] 87.8 Hz

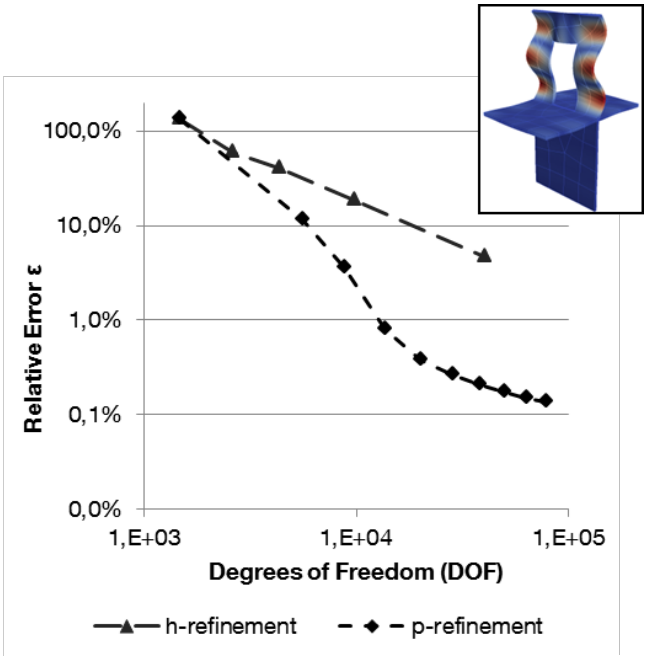

Figure 18: Mode [35] 165.7 Hz

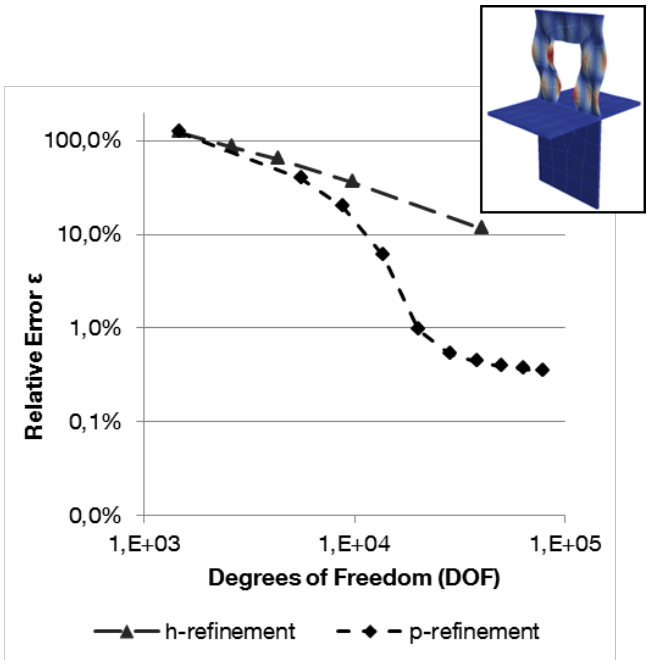

Figure 19: Mode [80] 317.6 Hz

A higher order, pre asymptotic convergence rate is observed with the p-version finite element method compared to the h-version.

For a comparison of the convergence behavior of the four frequency octave bands the average error within each band is formed and compared for p- and h-refinement strategies. The resulting convergence plots are shown in Figure 20. For all frequency bands the p-refinement strategy shows a superior performance of p-FEM to h-FEM.

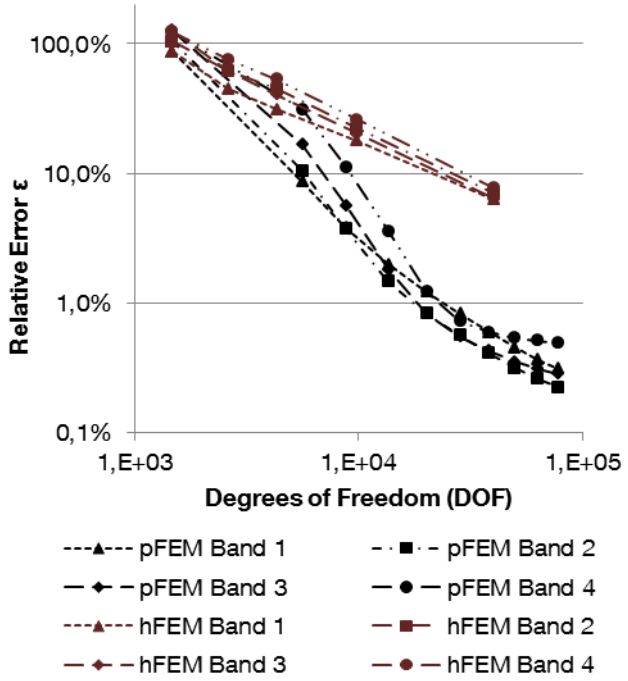

Figure 20: Convergence plots for p- vs. h-refinement of frequency octave bands.

CONCLUSION AND OUTLOOK

An exemplary simulation pipeline for vibro-acoustic analysis of laminated timber structures is presented. The high-order finite element method on truly solid hexahedral meshes is used for FEM modal analysis. The integration of this simulation pipeline into a planning process based on building information models is outlined. The numerical results demonstrate the potential of high-order finite elements in combination with proper mesh design for mid-frequency vibro-acoustics.

The presented modeling, meshing and simulation pipeline applies in principle for single laminated timber components as well as larger assemblies up to whole buildings. The extension of the numerical simulation pipeline presented in this contribution to non-conforming large scale models is one focus of our further research activities. Another focus will be the accurate description of weak acoustic connections of components in a non-conforming FE model.

Furthermore, the presented numeric results will be validated against experimental modal analysis of laminated timber constructions.

ACKNOWLEDGMENTS

The authors acknowledge the helpful discussions, in particular with Ulrich Schanda, Simon Mecking (HS Rosenheim), Martin Buchschmid, Christoph Winter (TU München) and Barbara Wohlmuth (TU München). The financial support provided by the AiF and DFG under grant No. RA 624/21-1 is gratefully acknowledged.

REFERENCES

[1] B.A. Szabó and I. Babuška, *Finite element analysis*, John Wiley & Sons, 1991.

[2] B.A. Szabó, A. Düster and E. Rank, *The p-version of the finite element method,* Encyclopedia of Computational Mechanics, John Wiley and Sons, 2004.

[3] F. Ihlenburg and I. Babuška, *Dispersion analysis and error estimation of Galerkin finite element methods for the numerical computation of waves*, Int. J. Numer. Methods Engrg. Vol. 38, pp. 3745–3774, 1995.

[4] S. Dey, *Evaluation of p-FEM approximations for mid-frequency elasto-acoustics*, J. Comput. Acoust. Vol. 11, pp. 195–225, 2003.

[5] A. Düster, H. Bröker and E. Rank, *The p-version of the finite element method for three-dimensional curved thin walled structures*, Int. J. Numer. Methods Engrg. Vol. 52, pp. 673-703, 2001.

[6] E. Rank, A. Düster, V. Nübel, K. Preusch and O.T. Bruhns, *High order finite elements for shells*, J. Comp. Methods in Applied Mechanics and Engrg., Vol. 194, pp. 2494-2512, 2005.

[7] A. Rabold, A. Düster and E. Rank, *FEM based prediction model for the impact sound level of floors*, Proc. EURONOISE, Paris, France, 2008

[8] A. Rabold, A. Düster, J. Hessinger and E. Rank, *Optimization of lightweight floors in the low frequency range with a FEM based prediction model*, Proc. DAGA, Rotterdam, Netherlands, 2009.

[9] F. Frischmann, S. Kollmannsberger and A. Rabold, *Prä-Prozessor Framework für BIM-gekoppelte vibroakustische Simulationen im Holzbau*, Proc. Forum Bauinformatik, Munich, Germany, 2013.

[10] C. Sorger, A. Düster and E. Rank, *Generation of curved high-order hexahedral finite element meshes for thin-walled structures*, Proc. 11th ISGG Conference, Montreal, Canada, 2009.

[11] C. Sorger, F. Frischmann, S. Kollmannsberger and E. Rank, *TUM.GeoFrame: automated high-order hexahedral mesh generation for shell-like structures*, J. Engineering with Computers, 2012.

[12] B. Flemisch, M. Kaltenbacher, S. Triebenbacher and B. Wohlmuth, *Applications of the Mortar Finite Element Method in Vibroacoustics and Flow Induced Noise Computations*, Acta Acustica united with Acustica. Vol. 96, pp. 96: 536-55, 2010.

[13] R. Craik and L. Galbrun, *Vibration transmission through a frame typical of timber-framed buildings*, J. of Sound and Vibration, Vol. 281, pp. 763-782, 2005.

[14] J-L. Kouyoumji, G. Borello and E. Thibier, *Sound Transmission Loss of Timber Construct., Measurem. and Modeling Using SEA-Wood, a Statistical Energy Analysis Software for Light Weight Constructions*, Proc. INTER-NOISE, Shanghai, China, 2008.

[15] *buildingSMART – International home of openBIM*. URL: http://www.buildingsmart.org

[16] *IfcPpenShell* – open source ifc geometric engine. URL: http://ifcopenshell.org/

[17] M. Kohrmann, M. Buchschmid, A. Greim, G. Müller, U. Schanda, *Vibroacoustic characteristics of light-weighted slabs – Part 1: Aspects of Numerical Modeling, Model Updating and Parametric Studies using the Buckingham Pi-Theorem*, Proc. DAGA, Mehran, Italy, 2013.

[18] M. Buchschmid, M. Kohrmann, C. Winter, R. Völtl, U. Schanda, G. Müller, *Vibroacoustic characteristics of light-weighted slabs – Part 2: Measurement-Based Investigation of the Sound Radiation of Suspended Ceilings*, Proc. DAGA, Mehran, Italy, 2013.